

Minimal QCDF Model for $B \rightarrow \pi K$ Puzzle

Tsung-Wen Yeh

*Department of Science Education and Application,
National Taichung University of Education, Taiwan, R.O.C.**

(Dated: March 3, 2022)

In this work, we propose a model by combining the parametrization method and the QCD factorization to study the $B \rightarrow \pi K$ puzzle. The parametrization for the $B \rightarrow \pi K$ amplitudes introduces twelve parameters, the weak angle γ and the other eleven hadronic parameters. These hadronic parameters are assumed to be perturbative and can be calculated by the QCD factorization (QCDF). The calculational accuracy of the QCDF is improved by including the twist-3 three parton tree and one loop corrections. Three additional nonperturbative strong phases from the gluonic penguin, color suppressed, and color favored tree diagrams are required to account for the direct CP asymmetries. The weak angle, three nonperturbative strong phases, and four scale variables are assumed as fitting parameters. Four scale variables represent the factorization scales for the decays, each decay mode with one scale. These eight parameters are determined by a least squares fit to the eight measurements for $B \rightarrow \pi K$ decays, four branching ratios and four direct CP asymmetries. The fit shows that the hadronic parameters need to be process-dependent. A large negative relative phase associated with the internal up quark gluonic penguin diagram is observed. The weak angle γ is found to be 72.1 ± 5.8 degree, being consistent with the world averaged value, 72.1 ± 5.8 degree. By a least squares fit to the mixing induced asymmetry $S(\pi^0 K_S) = 0.58 \pm 0.06$, the weak angle β is determined to be 22.9 ± 2.1 degree, which is in a well agreement with the world averaged value, $22.5 \pm 4.4 \pm 0.6$ degree. The model predicts the ratio C'/T' (color suppressed/color favored) to be 0.59 ± 0.08 . The above evidences indicate that the model can solve the $B \rightarrow \pi K$ puzzle consistently. The model is used to examine the quadrangle relation of the isospin symmetry assumed for the $B \rightarrow \pi K$ system. The ratio of the two sides of the quadrangle relation is calculated to be $(0.87 \pm 0.15) \exp(-i22^\circ)$, which signals the isospin symmetry breaking at 6σ . The process-dependent hadronic parameters break the isospin symmetry “dynamically”. The application of our method to other decay processes is straightforward.

PACS numbers: 12.15.Ff, 12.38.Bx, 12.39.St, 13.25.Hw, 14.40.Nd.

Keywords: perturbative QCD, factorization, isospin, B physics, CP violation, CKM mechanism.

I. INTRODUCTION

In order to establish the CKM mechanism of the Standard Model (SM), the studies of hadronic B decays have been devoted to construct the unitarity triangle $V_{ub}^* V_{ud} + V_{cb}^* V_{cd} + V_{tb}^* V_{td} = 0$, for which a systematic procedure has been developed [1, 2]. Experimentally, many rare processes have been measured by BABAR, Belle and LHCb[3]. The benchmarks are the mixing induced CP asymmetry $S(B \rightarrow J/\psi K) = 0.691 \pm 0.017$ and the direct CP asymmetry $A_{CP}(B^0 \rightarrow \pi^- K^+) = -0.082 \pm 0.006$ [4]. However, there appeared many difficulties in theories. One of these is the $B \rightarrow \pi K$ puzzle:

1. The theoretical predictions for the branching ratios are smaller than the experimental data [5–8].
2. The theoretical predictions for the CP asymmetries have a much different pattern from that of the experimental measurements [5–10].
3. It is difficult to reach consistent explanations for different experimental measurements [11–13].

At present, it seems still unable to solve the puzzle by model-independent methods [14], such as the flavor symmetry approach [11–13, 15, 16], or the global-fit approach [14, 15, 17–19]. The other possible method could be to employ the perturbative QCD (pQCD) theories [5–10]. In this work, QCD factorization (QCDF)[5, 20, 21] is employed to provide a calculational framework. The concern will focus on how to disentangle the weak phases from the strong phases. Specifically, a model based on a general parametrization for the $B \rightarrow \pi K$ decay amplitudes will be constructed. There will introduce eleven hadronic parameters to be calculated by the QCDF. Three additional nonperturbative strong phases, which are closely related to the direct CP asymmetries, are required to explain the experimental data.

In addition, the model assumes that the parameters could be process-dependent. The reason is easy to understand from the point of view of the pQCD approach. Any parameter is expressed as a convolution integral of the short and long distance parts. Although the long distance part is process-independent, however, the process-dependence of the short distance part makes the hadronic parameter to be process-dependent. This means that the value of any parameter for different processes would be different. We will show that this point is important to find a solution to the puzzle.

In past years, the QCDF calculations have considered

* twyeh@mail.ntcu.edu.tw

corrections up to twist-3 two parton and NNLO in α_s [5, 22–25]. These calculations show no significant enhancements in the predictions for the branching ratios and direct CP asymmetries [5]. Since the $B \rightarrow \pi K$ decays are penguin dominated, there are twist-3 chirally enhanced corrections from the effective operator $Q_{6,8}$, for which there also exist three parton contributions. As indicated in Ref.[26], the tree level three parton terms could significantly improve the predictions for branching ratios. In order to improve the calculational accuracy, we will calculate the three parton contributions up-to one loop radiative corrections.

The organization is as follows. In Sec.II, a general parametrization method for the amplitudes [27, 28] will be used to construct the model for the $B \rightarrow \pi K$ decays. The model contains twelve parameters: the weak angle γ and the other eleven parameters. An improved factorization formula up-to $O(\alpha_s^2/m_b)$ will be constructed by including the three parton corrections. The formula will be used to calculate the parameters in Sec.III. In Sec.IV, a fitting strategy will be developed to extract the weak and the strong phases from the data. According to the fitted result, the phenomenology analysis and discussions will be present in Sec.V. Conclusion will be given in Sec.VI.

II. MODEL

A. Parameterizations

In general, the amplitudes for $B \rightarrow \pi K$ decays with $B = B^\pm, B^0(\bar{B}^0)$, $K = K^\pm, K^0(\bar{K}^0)$, and $\pi = \pi^\pm, \pi^0$, could be parameterized as follows [5, 14, 27–29]

$$A(\pi^- \bar{K}^0) = P'(1 + \epsilon_a e^{i\phi_a} e^{-i\gamma}), \quad (1)$$

$$-\sqrt{2}A(\pi^0 K^-) = P'(1 + \epsilon_a e^{i\phi_a} e^{-i\gamma} - \epsilon_{3/2} e^{i\phi} (e^{-i\gamma} - q e^{i\omega})), \quad (2)$$

$$-A(\pi^+ K^-) = P'(1 + \epsilon_a e^{i\phi_a} e^{-i\gamma} - \epsilon_T e^{i\phi_T} (e^{-i\gamma} - q_C e^{i\omega_C})), \quad (3)$$

$$\begin{aligned} \sqrt{2}A(\pi^0 \bar{K}^0) = P'(1 + \epsilon_a e^{i\phi_a} e^{-i\gamma} \\ + (\epsilon_{3/2} e^{i\phi} - \epsilon_T e^{i\phi_T}) e^{-i\gamma} \\ + (\epsilon_T q_C e^{i(\phi_T + \omega_C)} - \epsilon_{3/2} q e^{i(\phi + \omega)})), \end{aligned} \quad (4)$$

where $A(\pi K)$ mean the amplitudes of $B \rightarrow \pi K$ decays. In the above expressions, the “unitarity triangle” has been used to translate the contributions from λ_t to the λ_u and λ_c terms, where $\lambda_q = V_{qb}^* V_{qd}$ for $q = u, c, t$. P' denotes the major penguin amplitude (containing λ_c). The weak angle $\gamma = \arg(V_{ub}^*)$ comes from the terms containing λ_u . The others are real parameters, $\epsilon_a, \epsilon_{3/2}, \epsilon_T, q$ and q_C and their associated strong phases $\phi_a, \phi, \phi_T, \omega, \omega_C$ [5]. The amplitudes for $B^{+,0}$ are obtained by replacing the weak angle γ by $-\gamma$. Some relative minor terms such as annihilation, exchange and penguin-annihilation terms have been neglected.

In Eqs.(1-5), the isospin symmetry is assumed. The initial B meson (B^-, \bar{B}^0) is of $I_B = -\frac{1}{2}$ state $|B(I =$

$-\frac{1}{2})\rangle$. The final (πK) state can be decomposed into the $I_{\pi K} = +\frac{1}{2}$ state $\langle \pi(I = 1)K(I = -\frac{1}{2})|$, the $I_{\pi K} = -\frac{1}{2}$ state $\langle \pi(I = 0)K(I = -\frac{1}{2})|$, and the $I = -\frac{3}{2}$ state $\langle \pi(I = -1)K(I = -\frac{1}{2})|$. The effective weak Hamiltonian has $\Delta I = 0$ and $\Delta I = 1$ operators, where $\Delta I \equiv |I_B - I_{\pi K}|$. Therefore, the matrix element $\langle \pi K | H_{eff} | B \rangle$ could be described by three isospin amplitudes $B_{1/2}, A_{1/2}$, and $A_{3/2}$, which correspond to $\Delta I = 0$ with $I_{\pi K} = -\frac{1}{2}$, $\Delta I = 1$ with $I_{\pi K} = +\frac{1}{2}$, $\Delta I = 1$ with $I_{\pi K} = -\frac{3}{2}$, respectively. The decay amplitudes are expressed as [14]

$$A(\pi^- \bar{K}^0) = B_{1/2} + A_{1/2} + A_{3/2}, \quad (5)$$

$$-\sqrt{2}A(\pi^0 K^-) = B_{1/2} + A_{1/2} - 2A_{3/2}, \quad (6)$$

$$-A(\pi^+ K^-) = B_{1/2} - A_{1/2} - A_{3/2}, \quad (7)$$

$$\sqrt{2}A(\pi^0 \bar{K}^0) = B_{1/2} - A_{1/2} + 2A_{3/2}, \quad (8)$$

from which the quadrangle relation [30, 31] is obtained

$$\begin{aligned} A(\pi^- \bar{K}^0) + \sqrt{2}A(\pi^0 K^-) \\ = A(\pi^+ K^-) + \sqrt{2}A(\pi^0 \bar{K}^0) \\ = 3A_{3/2}. \end{aligned} \quad (9)$$

These isospin amplitudes $B_{1/2}, A_{1/2}, A_{3/2}$ need to be process-independent. The same argument is applied to the eleven parameters, $P', \epsilon_a, \epsilon_{3/2}, \epsilon_T, q, q_C, \phi_a, \phi, \phi_T, \omega, \omega_C$. One should note that the isospin symmetry and the process-independence are closely correlated. It is interesting to examine whether the isospin symmetry could be preserved or broken, if the parameters are process-dependent. This will be made in latter text.

There are total twelve parameters to be determined, but we have only eight independent measurements, four sets of branching rates and asymmetries. (We identify the measurement for the mixing induced CP asymmetry $S_{\pi^0 K_S^0}$ as an independent test for the weak angle β and our model.) It is impossible to completely determine all the parameters. In the next section, the QCDF with three parton corrections is used to calculate the eleven hadronic parameters. Further more, the three phases ϕ_a, ϕ, ϕ_T are assumed to contain both perturbative and nonperturbative QCD contributions. The perturbative parts $\hat{\phi}_a, \hat{\phi}, \hat{\phi}_T$, are calculated by the QCDF formalism. The nonperturbative $\bar{\phi}_a, \bar{\phi}, \bar{\phi}_T$ are determined by a least squares fit to the experimental data. We will also assume that the factorization scale μ for four processes are different, $\mu_i, i = 1, \dots, 4$. Then, there are total eight parameters, $\bar{\phi}_a, \bar{\phi}, \bar{\phi}_T, \gamma$, and μ_i , which can be completely determined by eight measurements. We identify this model as the minimal QCDF model (MQCDF).

B. Observables

In order to explicitly explore how the puzzle would happen, every term is remained in the following expressions without applying any approximation. Using the

above parametrization for the amplitudes, the branching ratios are expressed as

$$Br(\pi^- K^0) = \Gamma_{B^-} P'^2 [1 + 2\epsilon_a \cos(\phi_a) \cos(\gamma) + \epsilon_a^2] \quad (10)$$

$$\begin{aligned} Br(\pi^0 K^-) = & \frac{1}{2} \Gamma_{B^-} P'^2 [1 + \epsilon_{3/2}^2 + \epsilon_a^2 + \epsilon_{3/2}^2 q^2 \quad (11) \\ & + 2\epsilon_a \cos(\phi_a) \cos(\gamma) - 2\epsilon_{3/2} \cos(\phi) \cos(\gamma) \\ & + 2\epsilon_{3/2} q \cos(\omega + \phi) - 2\epsilon_{3/2} \epsilon_a \cos(\phi - \phi_a) \\ & - 2\epsilon_{3/2}^2 q \cos(\omega) \cos(\gamma) \\ & + 2\epsilon_{3/2} \epsilon_a q \cos(\omega + \phi - \phi_a) \cos(\gamma)], \end{aligned}$$

$$\begin{aligned} Br(\pi^+ K^-) = & \Gamma_{B^0} P'^2 [1 + \epsilon_T^2 + \epsilon_a^2 + \epsilon_T^2 q^2 \quad (12) \\ & + 2\epsilon_a \cos(\phi_a) \cos(\gamma) - 2\epsilon_T \cos(\phi_T) \cos(\gamma) \\ & + 2\epsilon_T q \cos(\omega + \phi_T) - 2\epsilon_T \epsilon_a \cos(\phi_T - \phi_a) \\ & - 2\epsilon_T^2 q \cos(\omega) \cos(\gamma) \\ & + 2\epsilon_T \epsilon_a q \cos(\omega + \phi_T - \phi_a) \cos(\gamma)], \end{aligned}$$

$$\begin{aligned} Br(\pi^0 K^0) = & \frac{1}{2} \Gamma_{B^0} P'^2 [1 + \epsilon_a^2 + \epsilon_{3/2}^2 \quad (13) \\ & + \epsilon_{3/2}^2 q^2 + \epsilon_T^2 + \epsilon_T^2 q_C^2 \\ & + 2\epsilon_a \cos(\phi_a) \cos(\gamma) - 2\epsilon_{3/2} \cos(\phi) \cos(\gamma) \\ & - 2\epsilon_T \cos(\phi_T) \cos(\gamma) + 2\epsilon_{3/2} q \cos(\omega + \phi) \\ & - 2\epsilon_{3/2} \epsilon_a \cos(\phi - \phi_a) + 2\epsilon_T q_C \cos(\omega_C + \phi_T) \\ & - 2\epsilon_T \epsilon_a \cos(\phi_T - \phi_a) - 2\epsilon_{3/2}^2 q \cos(\omega) \cos(\gamma) \\ & - 2\epsilon_T^2 q_C \cos(\omega_C) \cos(\gamma) \\ & + 2\epsilon_{3/2} \epsilon_a q \cos(\omega + \phi - \phi_a) \cos(\gamma) \\ & + 2\epsilon_T \epsilon_a q_C \cos(\omega_C + \phi_T - \phi_a) \cos(\gamma)], \end{aligned}$$

and the direct CP asymmetries written as

$$A_{CP}(\pi^- K^0) = N(\pi^- K^0) \epsilon_a \sin(\phi_a) \sin(\gamma), \quad (14)$$

$$\begin{aligned} A_{CP}(\pi^0 K^-) = & N(\pi^0 K^-) \sin(\gamma) [\epsilon_a \sin(\phi_a) \quad (15) \\ & - \epsilon_{3/2} \sin(\phi) + \epsilon_{3/2}^2 q \sin(\omega) \\ & - \epsilon_a \epsilon_{3/2} q \sin(-\phi_a + \phi + \omega)], \end{aligned}$$

$$\begin{aligned} A_{CP}(\pi^+ K^-) = & N(\pi^+ K^-) \sin(\gamma) [\epsilon_a \sin(\phi_a) \quad (16) \\ & - \epsilon_T \sin(\phi_T) + \epsilon_T^2 q_C \sin(\omega_C) \\ & - \epsilon_a \epsilon_T q \sin(-\phi_a + \phi_T + \omega_C)], \end{aligned}$$

$$\begin{aligned} A_{CP}(\pi^0 K^0) = & N(\pi^0 K^0) \sin(\gamma) [\epsilon_a \sin(\phi_a) \quad (17) \\ & + (\epsilon_{3/2} \sin(\phi) - \epsilon_T \sin(\phi_T)) \\ & + (\epsilon_{3/2}^2 q \sin(\omega) + \epsilon_T^2 q_C \sin(\omega_C)) \\ & + \epsilon_a (\epsilon_{3/2} q \sin(-\phi_a + \phi + \omega) \\ & - \epsilon_T q_C \sin(-\phi_a + \phi_T + \omega_C)) \\ & - \epsilon_{3/2} (\epsilon_T q \sin(\phi - \phi_T + \omega) \\ & + \epsilon_T q_C \sin(-\phi + \phi_T + \omega_C))], \end{aligned}$$

where

$$N(\pi K) = \frac{2P'^2 \Gamma_B}{Br(\pi K)}.$$

The branching ratios are calculated according to

$$Br(B \rightarrow \pi K) = \frac{1}{2} \Gamma_B (|A(B \rightarrow \pi K)|^2 + |A(\bar{B} \rightarrow \pi K)|^2)$$

where

$$\Gamma_B = \frac{\tau_B}{16\pi m_B}.$$

According to the particle data group (PDG) definition [4], the CP asymmetry is defined by

$$A_{CP} = \frac{Br(\bar{B} \rightarrow \bar{f}) - Br(B \rightarrow f)}{Br(\bar{B} \rightarrow \bar{f}) + Br(B \rightarrow f)}.$$

Three ratios

$$R = \frac{Br(\pi^+ K^-) + Br(\pi^0 K^0)}{Br(\pi^- K^0) + Br(\pi^0 K^-)} \frac{\Gamma_{B^-}}{\Gamma_{B^0}}, \quad (18)$$

$$R_c = 2 \left[\frac{Br(B^- \rightarrow \pi^0 K^-)}{Br(B^- \rightarrow \pi^- \bar{K}^0)} \right], \quad (19)$$

$$R_n = \frac{1}{2} \left[\frac{Br(\bar{B}^0 \rightarrow \pi^- K^+)}{Br(\bar{B}^0 \rightarrow \pi^0 K^0)} \right], \quad (20)$$

have been widely used in literature as tests for the SM. The comparisons between the theoretical predictions and experimental data of these quantities are left to Sec.V.

III. CALCULATIONS

At the factorization scale $\mu \sim m_b$ (the bottom quark mass), the effective weak Hamiltonian for $B \rightarrow \pi K$ decays is given by [32, 33]

$$\begin{aligned} H_{eff} = & \frac{G_F}{\sqrt{2}} \sum_{p=u,c} \lambda_p [C_1(\mu) Q_1^p(\mu) + C_2(\mu) Q_2^p(\mu) \quad (21) \\ & + \sum_{i=3,\dots,10} C_i(\mu) Q_i(\mu) + C_{7\gamma}(\mu) Q_{7\gamma}(\mu) \\ & + C_{8G}(\mu) Q_{8G}(\mu)] + h.c. \end{aligned}$$

where $\lambda_p = V_{ps}^* V_{pb}$ is the product of CKM matrix elements. The local $\Delta B = 1$ four quark operators Q_i are defined as

$$Q_1^p = (\bar{s}_\alpha p_\alpha)_{(V-A)} (\bar{p}_\beta b_\beta)_{(V-A)}, \quad (22)$$

$$Q_2^p = (\bar{s}_\alpha p_\beta)_{(V-A)} (\bar{p}_\beta b_\alpha)_{(V-A)},$$

$$Q_{3,5} = (\bar{s}_\beta b_\beta)_{(V-A)} \sum_{q'} (\bar{q}'_\alpha q'_\alpha)_{(V \mp A)},$$

$$Q_{4,6} = (\bar{s}_\beta b_\alpha)_{(V-A)} \sum_{q'} (\bar{q}'_\alpha q'_\beta)_{(V \mp A)},$$

$$Q_{7,9} = \frac{3}{2} (\bar{s}_\beta b_\beta)_{(V-A)} \sum_{q'} e_{q'} (\bar{q}'_\alpha q'_\alpha)_{(V \pm A)},$$

$$Q_{8,10} = \frac{3}{2} (\bar{s}_\beta b_\alpha)_{(V-A)} \sum_{q'} e_{q'} (\bar{q}'_\alpha q'_\beta)_{(V \mp A)},$$

$$Q_{7\gamma} = -\frac{e}{8\pi^2} (\bar{q} \sigma^{\mu\nu} (1 + \gamma_5) b) F_{\mu\nu},$$

$$Q_{8G} = -\frac{g}{8\pi^2} m_b (\bar{q} \sigma^{\mu\nu} (1 + \gamma_5) b) G_{\mu\nu},$$

where $q' \in \{u, d, s, c, b\}$, α and β mean color indices, and $e_{q'} = 2/3(-1/3)$ for $u(d)$ type quarks. The Wilson coefficients $C_i(\mu)$ collect the radiative contributions between μ and M_W up to next-to-leading order (NLO) in α_s . The renormalization scheme is chosen as the minimal-subtraction (\overline{MS}) with $\Lambda_{\overline{MS}}^{(5)} = 0.225$ GeV. The C_i are calculated by the naive dimensional regularization (NDR).

Assume the naive factorization $\langle \pi K | Q_i(0) | B \rangle = \langle \pi | \bar{q}_1 \Gamma_{i,\mu} b | B \rangle \langle K | \bar{q}_2 \Gamma_i^\mu q_3 | 0 \rangle$ or $\langle K | \bar{q}_1 \Gamma_{i,\mu} b | B \rangle \langle \pi | \bar{q}_2 \Gamma_i^\mu q_3 | 0 \rangle$, with $\Gamma_{u,i} \otimes \Gamma_i^\mu = \gamma_\mu(1 - \gamma_5) \otimes \gamma^\mu(1 \pm \gamma_5)$, and include possible one loop radiative corrections to the factorized terms, the hadronic matrix element $\langle \pi K | Q_i(0) | B \rangle$ could be expressed in the following factorized form, up-to the twist-3 and NLO in α_s ,

$$\begin{aligned} & \langle \pi K | Q_i(0) | B \rangle \\ &= F_0^{B\pi}(0) \int_0^1 du \text{Tr}[T_{i,K}^I(u) \phi^K(u)] \\ &+ F_0^{BK}(0) \int_0^1 du \text{Tr}[T_{i,\pi}^I(u) \phi^\pi(u)] \\ &+ \int_0^\infty d\xi \int_0^1 du \int_0^1 dv \text{Tr}[\phi^B(\xi) T_{i,B\pi K}^{II}(\xi, u, v) \\ &\phi^\pi(u) \phi^K(v)] \end{aligned} \quad (23)$$

where Tr means the trace taken over the spin indices and the integrals are made over the momentum fractions u, v, ξ . The hard scattering kernels, $T^{I,II}$, describe the short distance interactions between partons of the external initial and final state mesons. The kernel T^I contains tree (T), vertex (V), and penguin (P) contributions. The kernel T^{II} contains hard spectator (HS). The transition form factors, $F_0^{B\pi}$ and F_0^{BK} , and the meson spin distribution amplitudes ϕ^B, ϕ^π, ϕ^K encode the long distance interactions of the quarks and gluons. The validity of the factorization formula is explained below.

The factorization at leading twist order has been well-known [5, 21]. In the following, let's concentrate on the twist-3 level.

At the twist-3 two parton order, the hard spectator terms may contain end-point divergences in the form

$$X_H = \int_0^1 du \frac{\phi_p(u)}{u}, \quad (24)$$

if the twist-3 two parton pseudo-scalar distribution amplitude ϕ_p is a constant [5, 21]. This viewpoint of a constant ϕ_p has been widely employed in literature. However, this is not the correct fact, because a constant ϕ_p is determined by the equation of motion (EOM) at the chiral symmetry breaking scale $\mu_c \sim 1$ GeV. The partons involving in the hard scattering kernels T^{II} would have energies about the energetic scale $\mu_E \sim m_b \gg \mu_c$. The correct EOM of ϕ_p would be taken at the energetic scale μ_E instead of μ_c . As a result, ϕ_p becomes equal to ϕ_σ and not a constant. The above mentioned end-point divergences in the hard spectator terms would vanish [26].

There also exist end-point divergences from the annihilation terms in the form

$$X_A = \int_0^1 du \frac{\phi_P(u)}{u(u-\xi)}, \quad (25)$$

even for the twist-2 pseudo-scalar distribution amplitude ϕ_P [5, 21]. The regularization method is not to neglect the momentum fraction factor ξ from the spectator lines of the B meson. It can be shown that the regularized result is equivalent to include the twist-4 contributions [34]. As a result, the annihilation terms up to twist-3 are also factorizable. The annihilation terms are not included in the above factorization formula and will be neglected in later calculations.

According to the study by Yeh [34], there are five types of different ways as shown in Fig.1 that the three parton state $|q\bar{q}g\rangle$ of the emitted final state meson $M = \pi, K$ can contribute at one loop level. The three parton state from the B meson needs not be considered, because only soft spectator gluonic partons can involve and their contributions are power suppressed by $O(1/m_B^2)$. By power counting [26], it is easy to see that only contributions from Fig. 1(a) are leading at twist-3 order (i.e., suppressed by $O(1/m_B)$) and the other types of contributions are at least of twist-4 (i.e., suppressed by $O(1/m_B^2)$) than the leading twist-2 term). Considering only contributions from Fig.1(a), the meson spin distribution amplitude $\phi^M(u)$ for $M = \pi, K$ has the following spin representation [26]

$$\begin{aligned} & \phi^M(u) \\ &= \int_0^\infty \frac{d\lambda}{2\pi} e^{-iu\lambda} \langle M | \bar{q}_a(0) q_b(\frac{\lambda}{E}n) | 0 \rangle \\ &+ \int_0^\infty \frac{d\lambda}{2\pi} \int_0^\infty \frac{d\eta}{2\pi} e^{-i\alpha\lambda} e^{-i\beta\eta} \langle M_2 | \bar{q}_a(0) i g A(\frac{\eta}{E}n) q_b(\frac{\lambda}{E}n) | 0 \rangle \\ &= -\frac{if_M}{4N_c} \left[\gamma_5 \not{q} \phi_P(u) + \mu_\chi \left(\gamma_5 \phi_p(u) - \frac{1}{2} \epsilon_\perp \cdot \sigma \phi_\sigma(u) \right. \right. \\ &\quad \left. \left. + 2\gamma_5 \delta(u - \alpha - \beta) \int_0^1 d\alpha \int_0^{(1-\alpha)} d\beta \frac{\phi_{3p}(\alpha, \beta)}{\alpha\beta} \right) \right] \end{aligned} \quad (26)$$

where $\epsilon_\perp \cdot \sigma = \epsilon_{\alpha\beta\eta\lambda} \sigma^{\alpha\beta} \bar{n}^\eta n^\lambda$ with \bar{n}^μ and n^μ being light like unit vector satisfying $\bar{n}^2 = n^2 = 0$ and $\bar{n} \cdot n = 1$. f_M is the decay constant and $\mu_\chi^M = m_M^2/(m_{q_a} + m_{q_b})$ is the chiral enhanced factor. ϕ_P is the twist-2 pseudo-scalar distribution function and ϕ_p and ϕ_σ are twist-3 two parton pseudo-scalar and pseudo-tensor distribution functions. The three parton distribution function ϕ_{3p} is defined by

$$\begin{aligned} & \int_0^\infty \frac{d\lambda}{2\pi} \int_0^\infty \frac{d\eta}{2\pi} e^{-i\alpha\lambda} e^{-i\beta\eta} \\ & \langle M_2 | \bar{q}(0) \gamma_5 \sigma^{\alpha\beta} g G^{\mu\nu}(\frac{\eta}{E}n) q(\frac{\lambda}{E}n) | 0 \rangle \\ &= -if_{M_2} \mu_\chi P^{\alpha\beta\mu\nu}(q) \phi_{3p}(\alpha, \beta) \end{aligned} \quad (27)$$

and has a parametrization

$$\phi_{3p}(\alpha, \beta) = 360\eta\alpha\beta^2(1 - \alpha - \beta)(1 + \frac{1}{2}\omega(7\beta - 3)) \quad (28)$$

with $\eta = 0.015$ and $\omega = -3$. This representation of the spin distribution ϕ^M is written according to the following facts:

- The effective spin structure and the integrals of ϕ_{3p} can be derived from the tree level Feynman diagrams similar to Fig.1(a), in which the radiative gluon is absorbed by the vertex. The detailed derivations refer to [26]. When the three parton one loop Feynman diagrams as depicted in Fig.1(a) are considered, it can be easily derived that the same spin structure is also applicable. Effectively, one may regard the three parton in this scenario as a pseudo-scalar two parton term. This shows a very convenient way to calculate the three parton one loop corrections by referring to those one loop calculations of ϕ_p [34].
- It can be shown that the energetic EOM $\phi_p = \phi_\sigma$ [26] would not change if ϕ_{3p} is considered. This is because the spin projector $P^{\alpha\beta\mu\nu}(q)$ vanishes at the energetic EOM condition. It implies that ϕ_p and ϕ_σ decouple from ϕ_{3p} at the energetic limit $E \gg \Lambda_{QCD}$.

Combining the above two facts, it can be shown that the one loop corrections of ϕ_{3p} are factorizable according to the analysis for the factorizability of the one loop corrections of ϕ_p given in [34]. The complete analysis of the above arguments will be present elsewhere. The B meson spin distribution amplitude is given by [34]

$$\begin{aligned} \phi^B(\xi) &= \int_0^\infty \frac{d\lambda}{2\pi} e^{-i\xi\lambda} \langle 0 | \bar{q}(0) b(\frac{\lambda}{E} n) | B \rangle \quad (29) \\ &= \frac{if_B}{4N_c} [(\not{P}_B + m_B) \gamma_5 \phi_B(\xi)] . \end{aligned}$$

For numeric calculations, we employ the following models

$$\phi_P(u) = \phi_p(u) = 6u(1-u), \quad (30)$$

$$\phi_B(\xi) = \frac{N_B \xi^2 \bar{\xi}^2}{[\xi^2 + \epsilon_B \bar{\xi}]^2}, \quad (31)$$

with $N_B = 0.133$, $\epsilon_B = 0.005$ for $\lambda_B = 350$ MeV. N_B and ϵ_B are determined by the moments

$$\int_0^1 d\xi \phi_B(\xi) = 1, \quad \int_0^1 d\xi \frac{\phi_B(\xi)}{\xi} = \frac{m_B}{\lambda_B}, \quad (32)$$

where the errors are controlled within 1%. Since the radiative corrections for the meson distribution amplitudes start at NNLO $O(\alpha_s^2)$, they could be neglected at NLO calculations.

Summarizing the above analysis, it shows that the factorization formula of QCDF given in Eq.(23) is valid up to complete twist-3 power corrections and NLO in α_s . Due to their smallness as compared with the other types of contributions, we will completely neglect the annihilation terms. This makes our later explanations for the puzzle completely different from most literature based on

QCDF, in which the annihilation electro-weak penguin terms would be important [5, 21].

In the following, the tree, vertex, penguin, and hard spectator contributions are collected as $a_i^p(\pi K)$ for each Q_i as given below

$$\begin{aligned} &a_i^p(\pi K, \mu) \quad (33) \\ &= (C_i(\mu) + \frac{C_{i\pm 1}(\mu)}{N_c}) N_i(K) \\ &+ \frac{C_{i\pm 1}(\mu)}{N_c} \frac{\alpha_s(\mu) C_F}{4\pi} [V_i^{(2)}(K) + V_i^{(3)}(K)] \\ &+ (4\pi\alpha_s(\mu) C_F) \frac{C_{i\pm 1}(\mu)}{N_c^2} [H_i^{(2)}(\pi K) + H_i^{(3)}(\pi K)] \\ &+ P_i^{p(2)}(K, \mu) + P_i^{p(3)}(K, \mu). \end{aligned}$$

The expressions for the tree $N_i(K)$, the two parton vertex $V_i^{(2)}(K)$, the two parton hard spectator $H_i^{(2)}(\pi K)$, and the two parton penguin $P_i^{p(2)}(K)$ are referred to [5, 34]. Here, we only present the three parton vertex $V_{6,8}^{(3)}(K)$, the three parton hard spectator $H_i^{(3)}(\pi K)$, and the three parton penguin $P_{6,8}^{p(3)}(K, \mu)$ as follows

$$\begin{aligned} &V_{6,8}^{(3)}(K) \quad (34) \\ &= 2 \int_0^1 d\alpha \int_0^{(1-\alpha)} d\beta \left[\frac{\phi_{3p}(\alpha, \beta) (-6 + h^{(3)}(\alpha, \beta))}{\alpha\beta} \right], \end{aligned}$$

where the kernel is

$$h^{(3)}(\alpha, \beta) = 2 \left[\text{Li}_2(x) + \frac{1}{2} (\ln \bar{x})^2 - (x \leftrightarrow (1-x)) \right]_{x=\alpha+\beta} \quad (35)$$

The penguin functions $P_{6,8}^{p(3)}(K, \mu)$ are given by

$$\begin{aligned} &P_6^{p(3)}(K, \mu) \quad (36) \\ &= \frac{\alpha_s(\mu) C_F}{4\pi N_c} \left\{ C_1(\mu) \left[\left(\frac{4}{3} \ln \frac{m_b}{\mu} + \frac{2}{3} \right) A_G - G_K^{(3)}(s_p) \right] \right. \\ &\quad + C_3(\mu) \left[2 \left(\frac{4}{3} \ln \frac{m_b}{\mu} + \frac{2}{3} \right) A_G - G_K^{(3)}(0) - G_K^{(3)}(1) \right] \\ &\quad + (C_4(\mu) + C_6(\mu)) \left[\frac{4}{3} n_f \left(\ln \frac{m_b}{\mu} \right) A_G \right. \\ &\quad \left. - (n_f - 2) G_K^{(3)}(0) - G_K^{(3)}(s_c) - G_K^{(3)}(1) \right] \\ &\quad \left. - 4C_{8g}^{\text{eff}} \int_0^1 d\alpha \int_0^{(1-\alpha)} d\beta \frac{\phi_{3p}(\alpha, \beta)}{\alpha\beta} \right\}, \\ &P_8^{p(3)}(\mu) \quad (37) \\ &= \frac{\alpha}{9\pi N_c} \left\{ (C_1(\mu) + N_c C_2(\mu)) \right. \\ &\quad \left[\frac{4}{3} A_G \ln \frac{m_b}{\mu} + \frac{2}{3} A_G - G_K^{(3)}(s_p) \right] \\ &\quad \left. - 6C_{7\gamma}^{\text{eff}} \int_0^1 d\alpha \int_0^{(1-\alpha)} d\beta \frac{\phi_{3p}(\alpha, \beta)}{\alpha\beta} \right\}, \end{aligned}$$

where $n_f = 5$ denotes the number of the flavors.

The functions $G_K^{(3)}(s_p)$ is defined as

$$\hat{G}_K^{(3)}(s_p) = 2 \int_0^1 d\alpha \int_0^{(1-\alpha)} d\beta \frac{\phi_{3p}(\alpha, \beta)}{\alpha\beta} G(s - i\epsilon, 1-x)|_{x=\alpha+\beta},$$

$$G(s, u) = -4 \int_0^1 dx x(1-x) \ln[s - x(1-x)u].$$

By substituting $s_p = 0, m_c^2/m_b^2, 1, \hat{G}_K^{(3)}(s_p)$ are calculated for later numerical analysis

$$\hat{G}_K^{(3)}(0) = 0.81 - i1.23,$$

$$\hat{G}_K^{(3)}(s_c) = 1.26 - i0.94,$$

$$\hat{G}_K^{(3)}(1) = 0.059.$$

The effective Wilson coefficients $C_{7\gamma}^{\text{eff}}$ and C_{8g}^{eff} are calculated at their leading order in α_s to be constants

$$C_{7\gamma}^{\text{eff}} = -0.32, \quad (38)$$

$$C_{8g}^{\text{eff}} = -0.15. \quad (39)$$

The hard spectator functions $H_i^{(3)}(\pi K)$ are, for $i = 1 - 5, 7, 9, 10$,

$$\begin{aligned} H_i^{(3)}(\pi K) & \quad (40) \\ = 2 \frac{B_{\pi K}}{A_{\pi K}} m_B r_\chi^\pi(\mu_h) \int_0^1 d\xi \frac{\phi_B(\xi)}{\xi} \int_0^1 d\alpha \int_0^{(1-\alpha)} d\beta \int_0^1 du \\ & \times \left[\frac{\phi_{3p}(\alpha, \beta) \phi_P(u)}{(\alpha + \beta) \alpha \beta (\bar{u} - \xi)} \right], \end{aligned}$$

where

$$B_{\pi K} = i \frac{G_F}{\sqrt{2}} f_B f_K f_\pi \quad (41)$$

and $H_{6,8}^{(2,3)}(\pi K) = 0$. The scale in $r_\chi^\pi(\mu_h)$ is assumed as $\mu_h = \sqrt{\Lambda_h \mu}$ and $\Lambda_h = 0.5 \text{ GeV}$.

According to the QCD factorization formula Eq.(1), we obtain the expressions for the amplitudes [5, 21, 34]

$$A(\pi^- \bar{K}^0) = \lambda_p A_{\pi K} \left[\left(a_4^p - \frac{1}{2} a_{10}^p \right) \right. \quad (42)$$

$$\left. + r_\chi^K \left(a_6^p - \frac{1}{2} a_8^p \right) \right],$$

$$\begin{aligned} -\sqrt{2} A(\pi^0 K^-) &= A_{\pi K} [\lambda_u a_1 + \lambda_p (a_4^p + a_{10}^p) \\ &+ \lambda_p r_\chi^K (a_6^p + a_8^p)] \\ &+ A_{K\pi} \left[\lambda_u a_2 + \lambda_p \frac{3}{2} (-a_7 + a_9) \right], \end{aligned} \quad (43)$$

$$\begin{aligned} -A(\pi^+ K^-) &= A_{\pi K} [\lambda_u a_1 + \lambda_p (a_4^p + a_{10}^p) \\ &+ \lambda_p r_\chi^K (a_6^p + a_8^p)], \end{aligned} \quad (44)$$

$$\begin{aligned} \sqrt{2} A(\pi^0 \bar{K}^0) &= \lambda_p A_{\pi K} \left[\left(a_4^p - \frac{1}{2} a_{10}^p \right) \right. \\ &+ r_\chi^K \left(a_6^p - \frac{1}{2} a_8^p \right) \\ &- A_{K\pi} \left[\lambda_u a_2 + \lambda_p \frac{3}{2} (-a_7 + a_9) \right], \end{aligned} \quad (45)$$

where the μ dependence of a_i is implicitly understood. We have defined the following factors

$$A_{\pi K} = i \frac{G_F}{\sqrt{2}} (m_B^2 - m_\pi^2) F_0^{B\pi}(m_K^2) f_K, \quad (46)$$

$$A_{K\pi} = i \frac{G_F}{\sqrt{2}} (m_B^2 - m_K^2) F_0^{BK}(m_\pi^2) f_\pi, \quad (47)$$

$$r_\chi^K = \frac{2m_K^2}{m_b(m_q + m_s)} (1 + A_G), \quad (48)$$

$$\lambda_u = \lambda_c \tan^2 \theta_c R_b e^{-i\gamma}, \quad (49)$$

$$\tan^2 \theta_c = \frac{\lambda^2}{1 - \lambda^2}, \quad (50)$$

$$R_b = \frac{1 - \lambda^2/2}{\lambda} \left| \frac{V_{ub}}{V_{cb}} \right|, \quad (51)$$

$$\lambda = |V_{us}|. \quad (52)$$

The three parton tree factor A_G comes from the integration [26]

$$A_G = 2 \int_0^1 d\alpha \int_0^{(1-\alpha)} d\beta \frac{\phi_{3p}(\alpha, \beta)}{\alpha\beta}. \quad (53)$$

By comparing expressions given in Eqs.(1-5) and Eqs.(42-45), the perturbative parts of the amplitude pa-

rameters are calculated to be [21]

$$P' = \lambda_c A_{\pi K} \left[\left(a_4^c - \frac{1}{2} a_{10}^c \right) + r_\chi^K \left(a_6^c - \frac{1}{2} a_8^c \right) \right], \quad (54)$$

$$\epsilon_a e^{i\hat{\phi}_a} = \epsilon_{KM} \frac{\left(a_4^u - \frac{1}{2} a_{10}^u \right) + r_\chi^K \left(a_6^u - \frac{1}{2} a_8^u \right)}{\left(a_4^c - \frac{1}{2} a_{10}^c \right) + r_\chi^K \left(a_6^c - \frac{1}{2} a_8^c \right)}, \quad (55)$$

$$\begin{aligned} \epsilon_{3/2} e^{i\hat{\phi}} &= -\epsilon_{KM} \\ &\times \frac{a_1 + R_{\pi K} a_2 + \frac{3}{2} (a_{10}^u + r_\chi^K a_8^u + R_{\pi K} (a_9 - a_7))}{\left(a_4^c - \frac{1}{2} a_{10}^c \right) + r_\chi^K \left(a_6^c - \frac{1}{2} a_8^c \right)}, \end{aligned} \quad (56)$$

$$\epsilon_T e^{i\hat{\phi}_T} = -\epsilon_{KM} \frac{a_1 + \frac{3}{2} (a_{10}^u + r_\chi^K a_8^u)}{\left(a_4^c - \frac{1}{2} a_{10}^c \right) + r_\chi^K \left(a_6^c - \frac{1}{2} a_8^c \right)}, \quad (57)$$

$$\begin{aligned} q e^{i\omega} &= -\frac{3}{2\epsilon_{KM}} \\ &\times \frac{a_{10}^c + r_\chi^K a_8^c + R_{\pi K} (a_9 - a_7)}{a_1 + R_{\pi K} a_2 + \frac{3}{2} (a_{10}^u + r_\chi^K a_8^u + R_{\pi K} (a_9 - a_7))}, \end{aligned} \quad (58)$$

$$q_C e^{i\omega_C} = -\frac{3}{2\epsilon_{KM}} \frac{a_{10}^c + r_\chi^K a_8^c}{a_1 + \frac{3}{2} (a_{10}^u + r_\chi^K a_8^u)}, \quad (59)$$

where the notations

$$R_{\pi K} = \frac{A_{K\pi}}{A_{\pi K}}, \quad \epsilon_{KM} = \frac{|\lambda_u|}{|\lambda_c|} \simeq \frac{\lambda^2}{2},$$

are defined.

The parameters would be process-dependent due to the scale μ of the a_i . The scale μ could be different from the assumed $\mu = m_b$ and also depends on the process. These complicate relations are represented by the μ_i with i as an index for a specific process. Therefore, these parameters are interpreted as functions of μ_i and calculated through the above equations Eqs.(54-59). In this work, we will assume that P , ϵ_a , $\epsilon_{3/2}$, ϵ_T , q and q_C , ω , and ω_C are pure perturbative and allow ϕ_a , ϕ , and ϕ_T to contain both perturbative parts, $\hat{\phi}_a$, $\hat{\phi}$, and $\hat{\phi}_T$, and nonperturbative parts, $\bar{\phi}_a$, $\bar{\phi}$, and $\bar{\phi}_T$:

$$\begin{aligned} \phi_a &= \hat{\phi}_a + \bar{\phi}_a, \\ \phi &= \hat{\phi} + \bar{\phi}, \\ \phi_T &= \hat{\phi}_T + \bar{\phi}_T. \end{aligned}$$

This is because only ϕ_a , ϕ , and ϕ_T can directly involve in the direct CP asymmetries.

IV. ANALYSIS

In order to determine the eight parameters, γ , $\bar{\phi}_a$, $\bar{\phi}$, and $\bar{\phi}_T$, and μ_i with $i = 1, \dots, 4$, introduced in the above, we employ the following fitting procedure by using the eight measurements of four branching ratios and four direct CP asymmetries. The input data given in Table I are used to calculate the amplitude parameters given in Eqs.(54-59), which are then substituted into the Eqs.(10-17). The data are separated into four sets, one set for one process. Each set contains one branching ratio

and one asymmetry: Set-1: $Br(\pi^- \bar{K}^0)$ and $A_{CP}(\pi^- K_s^0)$; Set-2: $Br(\pi^0 K^-)$ and $A_{CP}(\pi^0 K^-)$; Set-3: $Br(\pi^+ K^-)$ and $A_{CP}(\pi^+ K^-)$; Set-4: $Br(\pi^0 \bar{K}^0)$ and $A_{CP}(\pi^0 K^0)$. Their experimental data are present in Table IV, in which only the PDG2016 data [4] are used and the HFAG2016 data [35] are listed for reference. The least squares fit method is used. The χ^2 function is defined as

$$\chi_i^2(\vec{\theta}) = \sum_{j=1}^2 \frac{(O_{ij}^{exp} - O_{ij}^{th}(\vec{\theta}))^2}{\sigma_{ij}^2}, \quad (60)$$

$$\chi_{tot}^2(\vec{\theta}) = \sum_{i=1}^4 \chi_i^2(\vec{\theta}), \quad (61)$$

where χ_i^2 is the χ^2 function for the i -th set of data: $i = 1$ for $B^- \rightarrow \pi^- \bar{K}^0$, $i = 2$ for $B^- \rightarrow \pi^0 K^-$, $i = 3$ for $\bar{B}^0 \rightarrow \pi^+ K^-$ and $i = 4$ for $\bar{B}^0 \rightarrow \pi^0 \bar{K}^0$. The fitting parameters are $\vec{\theta} = (\mu_i, i = 1, \dots, 4; \gamma, \bar{\phi}_a, \bar{\phi}, \bar{\phi}_T)$. The scale variable μ_i is defined for i -th data set. The experimental measurements O_{ij}^{exp} , the theoretical predictions O_{ij}^{th} , and the experimental errors σ_{ij} are for the j -th measurement of the i -th data set, $j = 1$ for the branching rate and $j = 2$ for the asymmetry. For each fitting procedure, only two measurements and one fitting parameter are used. The degree of freedom is equal to one. However, the nonlinear functional form of the expressions for the branching ratios and the asymmetries makes the fitting to be a nonlinear fit problem. It is not appropriate by using the standard least χ^2 fit method, in which all the parameters are simultaneously determined by calculating the best-fit value of the χ^2 function. To improve the task of fitting, we design the following iterative strategy similar to the Marquardt method [36]. The value of $\chi^2 = \chi_i^2, \chi_{tot}^2$ for each fitting procedure is very close to zero, $\chi^2 \simeq 0$.

A. Fitting Strategy

The following fitting strategy is employed to determine γ , $\bar{\phi}_a$, $\bar{\phi}$, $\bar{\phi}_T$ and μ_i , $i = 1, \dots, 4$.

1. Choose a reference value γ_{init} for the weak angle γ . Here, $\gamma_{init} = 72.1^\circ$ is chosen for the world averaged value $(72.1_{-5.8}^{+5.4})^\circ$ [35].
2. Calculate the χ^2 value for the data set $i = 1, \dots, 4$ by varying the factorization scale variable μ_i within the range $m_b/2 \leq \mu_i \leq 2m_b$ to find a least $\chi_{i,\mu}^2$ at the temporal μ_i^T .
3. Calculate the χ^2 value for the data set i by varying one of the strong phase variables $\bar{\phi}_a, \bar{\phi}, \bar{\phi}_T$ within the range $-180^\circ \leq \bar{\phi}_a, \bar{\phi}, \bar{\phi}_T \leq 180^\circ$ with the previous temporal μ_i^T to find a least $\chi_{i,\phi}^2$ at the temporal $\bar{\phi}_{a,i}^T, \bar{\phi}_i^T, \bar{\phi}_{T,i}^T$.
4. Repeat procedures 3 and 4 until $\chi_{i,\mu}^2 = \chi_{i,\phi}^2$ and obtain the fitted values of $\mu_i, \bar{\phi}_{a,i}, \bar{\phi}_i, \bar{\phi}_{T,i}$.

5. The fitted values of $\mu_i, \bar{\phi}_{a,i}, \bar{\phi}_i, \bar{\phi}_{T,i}$ are used to calculate the least χ^2 for all data by varying $-180^\circ \leq \gamma \leq 180^\circ$ to find a least χ_{tot}^2 at γ_{fit} .
6. Use γ_{fit} to repeat procedures 2-6 until the χ_{tot}^2 reaches a stable least value.
7. Use the criteria $\chi^2 \leq \sqrt{2\nu}$ to set the upper and lower bounds of each parameter. ν is the degree of freedom of the used data points and defined as $\nu = N - n$ with N the number of data point and n the number of the fitting parameters. For the procedures 3 and 4, $N = 2$ and $n = 1$ and $\nu = 1$. The bounds of γ_{fit} are determined by using $\chi^2 \leq \sqrt{2\nu}$ for $\nu = N - n = 4$ with $N = 8$ and $n = 4$.

B. Fitted Results

The fitted results for $\mu_i, \bar{\phi}_a, \bar{\phi}, \bar{\phi}_T$ and γ are listed in the TableII. The parameters calculated at μ_i are list in TableIII. For comparison, the parameters calculated for $m_b/2 \leq \mu \leq 2m_b$ with its central value at $\mu = \mu_0 = m_b$ are also listed (denoted as μ_0) in the same table. The fitted scales μ_i are used to calculate the averaged scale μ_{av} . (See below explanation for μ_{av} .) The predictions of QCDF for branching ratios and asymmetries are calculated at $m_b/2 \leq \mu \leq 2m_b$ and $\mu = \mu_{av} \pm \sigma_{av}$, denoted as Naive and Improved columns in Table IV. Using the fitted parameters to calculate the predictions for the branching ratios and asymmetries are given in the Fit column in TableIV, where the first errors are from μ_i and the second errors from the phase factors, $\bar{\phi}_a, \bar{\phi}, \bar{\phi}_T$. For comparisons, the S4 column in TableIV are quoted from Ref.[21], in which the predictions are calculated at the twist-3 two parton and NLO in α_s order in the S4 scenario.

Comments of the above analysis are given as follows.

- In QCDF, the factorization scale μ separates the perturbative physics from the nonperturbative. Priority, it is not possible to guest what scale is appropriate for a process. In the B decays, $\mu = m_b$ is a convenient but not absolute choice. Any μ within the range $m_b/2 \leq \mu \leq 2m_b$ is allowable. According to the fit result, different processes require different factorization scales.
- The branching ratios are sensitive to the factorization scale μ , while the asymmetries are sensitive to the strong phases ϕ_a, ϕ , and ϕ_T .
- The predictions for branching ratios with $m_b/2 \leq \mu \leq 2m_b$ can cover the experimental data within errors.
- The predictions for $A_{CP}(B^- \rightarrow \pi^- K_s^0)$ and $A_{CP}(\bar{B}^0 \rightarrow \pi^+ K^-)$ are in opposite sign to the data, and the predictions for $A_{CP}(B^- \rightarrow \pi^0 K^-)$ and $A_{CP}(\bar{B}^0 \rightarrow \pi^0 K^0)$ are in the same sign to the data.

- The predictions for four asymmetries have consistent magnitudes with the experimental data.
- The perturbative parts of ϕ_a, ϕ , and ϕ_T are in opposite sign to their nonperturbative parts.
- The experimental data favor a large negative ϕ_a and moderate negative ϕ and moderate positive ϕ_T . Especially, $\bar{B}^0 \rightarrow \pi^0 K^0$ mode favors $\phi \lesssim \phi_T$ to compensate $\epsilon_{3/2} \gtrsim \epsilon_T$.
- The major uncertainties come from the $A_{CP}(B^- \rightarrow \pi^- K^0)$ for $\bar{\phi}_a$ and $A_{CP}(\bar{B}^0 \rightarrow \pi^0 K^0)$ for $\bar{\phi}$ and $\bar{\phi}_T$. However, the more accurate asymmetries $A_{CP}(B^- \rightarrow \pi^0 K^-)$ and $A_{CP}(\bar{B}^0 \rightarrow \pi^+ K^-)$ require $\bar{\phi}_a, \bar{\phi}$, and $\bar{\phi}_T$ being process-dependent.
- $\bar{\phi}_a$ is determined by data set 1 and needs specific values for the data sets 2, 3, 4, respectively.
- $\bar{\phi}$ and $\bar{\phi}_T$ are equal and determined by data set 4 and they need specific values for the data sets 2 and 3.
- The better parametrization would be $\Phi_a = \bar{\phi}_a - \gamma$, $\Phi = \bar{\phi} - \gamma$, and $\Phi_T = \bar{\phi}_T - \gamma$. This allows for further exploration of the NP effects.
- Only uncertainties from the scale variables are taken as theoretical errors. The uncertainties from the input data are completely neglected.

V. DISCUSSIONS

To examine whether the puzzle could be resolved in our approach, we choose the following topics to discuss.

A. Basic Results

a. Fitting The fit of each data set gives $\chi^2 \simeq 0$ for one degree of freedom ($\nu = 1$). According to the least squares method (see e.g. [37]), a very small $\chi^2 \ll 1$ could mean either (i) our model is valid, or (ii) the experimental errors are too large, or (iii) the data is too good to be true. Since a poor model can only increase χ^2 , a too-small value of χ^2 cannot be indicative of a poor model. This implies that our model could be a good model for the data. The fitted results show that (i) the factorization scale variable μ is process-dependent, (ii) the strong phase variables ϕ_a, ϕ, ϕ_T are process-dependent. As a result, the eleven parameters are process-dependent as shown in Table III. This observation is in contradiction to the usual assumption that these parameters are process-independent. If this founding that the parameters are process-dependent is true, then the puzzle found by assuming the parameters to be process-independent would be questionable.

b. Averaged Analysis From Table II, the factorization scales μ_i of four processes are averaged as $\mu_{av} = 4.96 \pm 1.44 \text{ GeV}$, where the averaged factorization scale $\mu_{av} \pm \sigma_{av}$ is calculated by means of the weighted mean method

$$\mu_{av} = \frac{\sum_i \sigma_i \mu_i}{\sum_i \sigma_i}, \quad \sigma_{av} = \left(\frac{1}{\sum_i \sigma_i^2} \right)^{1/2}. \quad (62)$$

The μ_{av} denotes the specific energy scale relevant to the $B \rightarrow \pi K$ decays. For distinguishing, we call the parameters calculated by $\mu_0 = m_b$ as the “Naive” predictions and those calculated at μ_{av} as the “Improved” predictions. The uncertainties of μ_{av} come from the experimental data and those of μ_0 from the assumption of QCDF. The μ_{av} is more appropriate than by comparing their predictions with the corresponding data as given in Table IV. The parameters calculated at $\mu_{av} \pm \sigma_{av}$ are present in the column μ_{av} of Table III.

c. Three Parton Effects For comparison, the amplitude parameters with twist-3 three parton NLO corrections calculated in this work and similar terms with the twist-3 two parton NLO corrections calculated in Ref. [5] are present in the second column and the third column of Table III. Only P' , ϵ_T , q_C , and ω_C have significant differences between twist-3 two parton and twist-3 three parton calculations. The three parton penguin term $P^{(3)} = 51.4 \text{ eV}$ has about 15.5% enhancement than the two parton $P^{(2)} = 44.5 \text{ eV}$. The most significant difference comes from the ϵ_T . The three parton $\epsilon_T^{(3)} = 14.6(\%)$ is about two third of the two parton $\epsilon_T^{(2)} = 22.0(\%)$. This can be easily understood due to the enhanced effects from the three parton corrections, the denominator of Eq.(57) contains $r_\chi(a_6 - \frac{1}{2}a_8)$. The ratio $r = (\epsilon_{3/2} - \epsilon_T)/\epsilon_T \sim C'/T'$ has been suggested to be an important index for distinguishing whether SM can or can not explain the puzzle. Let's compare the theoretically predicted values: the naive $\epsilon_{3/2}(\%) = (22.7 \pm 7.0)_{th}$ and $\epsilon_T(\%) = (14.6 \pm 4.0)_{th}$, the improved $\epsilon_{3/2}(\%) = (24.2 \pm 3.0)_{th}$ and $\epsilon_T(\%) = (15.4 \pm 1.8)_{th}$, and the fit values, $\epsilon_{3/2}(\%) = (24.3 \pm 1.1)_{fit}$ and $\epsilon_T(\%) = (15.4 \pm 0.6)_{fit}$, which result in

$$\begin{aligned} r_{fit} &\simeq (0.59 \pm 0.08)_{fit} \\ r_{th} &= (0.55 \pm 0.57)_{th} (Naive) \\ r'_{th} &= (0.57 \pm 0.24)_{th} (Improved) \end{aligned}$$

The Naive r_{th} , the improved r'_{th} , and the fit r_{fit} imply that SM can explain the puzzle at 1σ , 2σ and 7.4σ , respectively. For reference, the two parton prediction gives $r^{(2)} \simeq 0.2$ as calculated from the second column of Table III, the values quoted from Ref. [5].

As for q , the three parton $q^{(3)} = 0.33$ is about four times the two parton $q^{(2)} = 0.083$. The three parton predictions can accommodate the data without additional EW penguin contributions from other sources as the two parton predictions required. On the other hand, the three parton $\omega_C^{(3)} = -7.9^\circ$ is about one sixth of the two parton $\omega_C^{(2)} = -54^\circ$.

The enhancements of the predictions for the branching ratios by the three parton corrections could be seen by comparing the Improved and the S4 columns in Table IV. The S4 predictions quoted from [5] are calculated at the twist-3 two parton order in the S4 scenario.

B. Predictions

a. Power Counting Puzzle In literature, the simple version of the $B \rightarrow \pi K$ puzzle is based on the analysis for the predictions of the SM by means of a power counting of the amplitude parameters [19, 27, 38, 39]. Under the standard parametrization of the CKM matrix elements, we have $\lambda_u \sim O(\lambda^4)$ and $\lambda_c \sim O(\lambda^2)$, where $\lambda = 0.22$ is the sine of the Cabibbo angle. If the $SU(3)$ flavor symmetry is valid, then we have $\epsilon_a \sim \epsilon_{KM} \sim O(\lambda^2)$, $\epsilon_{3/2} \sim \epsilon_T \sim O(\lambda)$, $q \sim q_C \sim 1$, $\epsilon_{3/2} - \epsilon_T \sim O(\lambda^2)$ [19, 27, 38, 39]. Combining these facts, we have the following Standard Model (SM) predictions $A_{CP}(B^- \rightarrow \pi^0 K^-) = A_{CP}(\bar{B}^0 \rightarrow \pi^+ K^-) \sim O(\lambda)$ and a vanishing $\Delta_{th} A_{CP} = 0$ up-to $O(\lambda^2)$, if the strong phases are of similar orders, $\phi \sim \phi_T$, $\omega \sim \omega_C$ [11].

Because the ΔA_{CP} is about $O(\lambda)$, at which SM predicts a vanishing ΔA_{CP} with errors $O(\lambda^2)$. However, the direct CP asymmetries of four processes are all of $O(\lambda^2)$. Therefore, in order to reveal the mystery of the puzzle, it needs the calculation accuracy up-to $O(\lambda^2)$.

By order of magnitudes, the twist-3 power corrections are of $O(\Lambda/m_B) \sim O(\lambda^2)$ and the NLO α_s corrections are of $O(\alpha_s^2(m_b)) \sim O(\lambda^2)$. This implies that QCDF with complete twist-3 power corrections and NLO corrections has the precision of $O(\lambda^2)$. That ensures that our calculations are able to distinguish the different terms of the asymmetries. As a result, we may be able to figure out the crucial differences which lead to the puzzle.

To make the above explanation clear, let's separately calculate the four terms in the square bracket of each direct CP asymmetry in Eqs. (14-17). The results are present in Table V, the columns 1, \dots , 4, denote the j-th term of each A_{CP} equation. For $A_{CP}(\pi^0 K^0)$, the terms are separated by different lines. The fourth term contains the last four terms. Now, we may understand why the puzzle may not exist:

1. Although ϵ_a is much smaller than P' , but it should not be neglected for A_{CP} .
2. Most of the first and second terms are of $O(\lambda^2)$ and the third and fourth terms of $O(\lambda^3)$. The largest term is $-\epsilon_{3/2} \sin(\phi) \sin(\gamma)$ of $A_{CP}(\pi^0 K^-)$. The second large term is $-\epsilon_T \sin(\phi_T) \sin(\gamma)$ of $A_{CP}(\pi^+ K^-)$. Both terms have different signs and magnitudes.
3. The puzzle assumes $N_2 = N_3 = 2$, but, in fact, $N_2 = 1.65$ and $N_3 = 1.94$.
4. The puzzle requires $|\epsilon_{3/2} - \epsilon_T| \sim O(\lambda^2)$. On the other hand, the data favor $|\epsilon_{3/2} - \epsilon_T| \sim O(\lambda)$.

In summary, the power counting can only differentiate $O(\lambda)$ and can not correctly distinguish the signs of the parameters. The $SU(3)_f$ needs to be broken to explain the $\Delta A_{CP} \neq 0$, which comes from the largest terms of $A_{CP}(\pi^0 K^-)$ and $A_{CP}(\pi^+ K^-)$ being unequal and in opposite signs.

b. Mixing Induced CP Asymmetry We now test MQCDF model by the mixing induced CP asymmetry $S_{\pi^0 K_S} = 0.58 \pm 0.06$ [4]. Under the invariance of CPT, the time dependent CP asymmetry $A_{CP}(t)$ for $\bar{B}^0 \rightarrow \pi^0 K^0$ is given by [4]

$$A_{CP}(t) = \frac{\Gamma_{\bar{B} \rightarrow f}(t) - \Gamma_{B^0 \rightarrow f}(t)}{\Gamma_{\bar{B} \rightarrow f}(t) + \Gamma_{B^0 \rightarrow f}(t)} \quad (63)$$

$$= \frac{-C_f \cos(\Delta m_d t) + S_f \sin(\Delta m_d t)}{\cosh(\frac{\Delta \Gamma_d}{2} t) + A_f^{\Delta \Gamma} \sinh(\frac{\Delta \Gamma_d}{2} t)},$$

where the $B^0 - \bar{B}^0$ system has mass difference Δm_d and width difference $\Delta \Gamma_d$ for the mass eigenstate $|B^0\rangle$ and $|\bar{B}^0\rangle$. The quantities are given by

$$C_f = \frac{1 - |\lambda_f|^2}{1 + |\lambda_f|^2}, \quad (64)$$

$$S_f = \frac{2\text{Im}(\lambda_f)}{1 + |\lambda_f|^2}, \quad (65)$$

$$A_f^{\Delta \Gamma} = -\frac{2\text{Re}(\lambda_f)}{1 + |\lambda_f|^2}, \quad (66)$$

where λ_f is defined as

$$\lambda_f = -e^{-2i\beta} \left[\frac{(1 + \epsilon_a e^{i\phi_a} e^{-i\gamma} + (\epsilon_{3/2} e^{i\phi} - \epsilon_T e^{i\phi_T}) e^{-i\gamma} + (\epsilon_T q C e^{i(\phi_T + \omega_C)} - \epsilon_{3/2} q e^{i(\phi + \omega)}))}{(1 + \epsilon_a e^{i\phi_a} e^{i\gamma} + (\epsilon_{3/2} e^{i\phi} - \epsilon_T e^{i\phi_T}) e^{i\gamma} + (\epsilon_T q C e^{i(\phi_T + \omega_C)} - \epsilon_{3/2} q e^{i(\phi + \omega)}))} \right]. \quad (67)$$

The best-fit results are as follows:

1. By using the world averaged $\beta = (22.5 \pm 4.4 \pm 1.2 \pm 0.6)^\circ$, the calculations give $S_f = 0.57 \pm 0.13$ and $C_f = -0.01$ and $A_f^{\Delta \Gamma} = 0.82 \pm 0.09$.
2. By using the above expression and the fitted parameters for $\pi^0 K_S$ mode given in the column μ_4 of Table III, the fit to $S_f = 0.58 \pm 0.06$ gives $\beta = (22.92_{-2.13}^{+2.08})^\circ$, which is in agreement with the world averaged $\beta = (22.5 \pm 4.4 \pm 1.2 \pm 0.6)^\circ$.

It implies that $S_{\pi^0 K_S} = 0.58 \pm 0.06$ and $\beta = (22.5 \pm 4.4 \pm 1.2 \pm 0.6)^\circ$ are consistent according to the MQCDF model.

c. Ratios of Modes Three ratios, R , R_c and R_n have been widely used for demonstration of the $B \rightarrow \pi K$ puzzle. We now compare their theoretical (R^{th} in the Improved column) and experimental values (R^{exp} in the 2016 column) in Table VI, which are calculated according to the Improved column in Table IV and the experimental data, respectively.

From the above calculations, we may notice the following interesting points:

1. For the ratio R , the central value of the predicted value $R^{th} = 0.91$ is very close to that of the experimental value $R^{exp} = 0.89$ within 3%.
2. The ratio of central values show $R_n^{th}/R_c^{th} \simeq 1 + 0.9\%$ and $R_n^{exp}/R_c^{exp} = 1 + 9.2\%$. Both are compatible within 10% despite of their respective uncertainties. The discussion about the 10% difference is left to the Sec. VI.

In summary, the comparisons between the theoretical predictions of this work and the experimental data for

these three ratios show no similar large discrepancies as claimed in [11–13].

C. Comparisons With Other Approaches

a. Flavor Symmetry Approach Many studies have employed the flavor symmetry approach [11–16, 29, 38, 40–44], which is an extension of the isospin symmetry approach. The amplitudes are expressed in terms of parameters which satisfy the symmetry. To conserve the symmetry, the parameters would be process-independent. By means of many sophisticated arguments, many important insights for the flavor physics have been derived. The arguments heavily rely on the assumption that the common parameters involved in different processes are universal such that they can be used for predictions. However, these arguments would be questionable if the parameters are process-dependent according to our finding in this work.

b. Global-Fit Approach In literature, there are studies [17–19] by employing the global-fit for analysis of the $B \rightarrow \pi K$ puzzle. The basic assumption of this fitting approach is that there would exist some symmetries such that the amplitudes can be parameterized in terms of universal parameters. However, this method has its intrinsic uncertainties. Since there may exist many (perhaps infinite) possible best-fit results, it is difficult to distinguish which result is the correct one. In addition, it is difficult to explain the underlying physics for the best-fit results. In our approach, there is no such problem.

c. NLO PQCD Approach Similar studies have been made by employing the PQCD approach [7–9]. The complete NLO calculations [8] are improved than the par-

tial NLO ones [9]. The complete NLO predictions [8] for the branching ratios and direct CP asymmetries are compatible with the experimental data. The authors of Ref. [7] indicated that some nonperturbative strong phase from the Glauber gluons are necessary. Although the QCDF and the PQCD approaches are based on different factorization assumptions, their calculations up to NLO and twist-3 order agree within theoretical uncertainties. This can be seen by comparing the Improved and PQCD columns in Table IV.

d. Final State Interactions The final state interactions of the $B \rightarrow \pi K$ decays are introduced to account for strong phases (see e.g. [45]). This approach uses the QCDF predictions as the reference by adding the final state interaction effects. The final state interactions occur through long distance inferences between different final states. The calculations introduce nonperturbative parameters which are determined by a best-fit to the data. Since the QCDF calculations contain final state interactions in the a_i functions, there would exist double counting effects in this approach [21]. On the other hand, our model has avoided this problem.

e. Endpoint Divergences There exist endpoint divergent terms in the standard QCDF calculations. To regularize the divergences, the following model is introduced [21]

$$X_A = (1 + \rho_A e^{i\phi_A}) \ln\left(\frac{m_B}{\Lambda_h}\right); \quad \rho_A \leq 1, \quad \Lambda_h = 0.5 \text{ GeV}.$$

The parameters ρ_A and ϕ_A are determined by a global-fit to the data. Because the factorization formula Eq.(23) is free from these end-point divergences [34], no such terms need to be considered in our calculations. Since the phase ϕ_A is associated with the annihilation terms, the explanations for the puzzle are different from ours.

D. Isospin Symmetry Breaking

a. Broken Isospin Symmetry The isospin symmetry is conserved under the weak interactions. If the isospin symmetry is also conserved by the QCD, then the $B \rightarrow \pi K$ amplitudes would obey the quadrangle relation Eq.(9) [30, 39]. This relation leads to the ratio $R_c/R_n = 1$, which is shown by the central value of the QCDF prediction (the Improved) $R_c/R_n \simeq 1$ in Table VI. However, the central values of the last experimental data show that $R_c/R_n = 1.1 > 1$. How does this imply for the quadrangle relation? To answer this, we may calculate the following ratio for the amplitudes listed in Table VII

$$r = \frac{A(\pi^- K^0) + \sqrt{2}A(\pi^0 K^-)}{A(\pi^- K^+) + \sqrt{2}A(\pi^0 K^0)} = \frac{A_{3/2}(B^-)}{A_{3/2}(\bar{B}^0)}, \quad (68)$$

$$r_{exp} = (0.87 \pm 0.15)e^{-i23^\circ}, \quad (69)$$

$$r_{th} = (1.04 \pm 1.0)e^{i0.4^\circ}, \quad (70)$$

where r_{exp} is calculated by the Fit column in Table VII and the r_{th} is calculated by the Improved column in the

same table. The experimental data imply that the amplitudes would not obey the quadrangle relation. It is in contradiction to the theoretical assumption, $r_{exp} \neq r_{th}$. Within uncertainties, we obtain $r_{exp} \neq 1$ at 6σ significance. That is $A_{3/2}(B^-) \neq A_{3/2}(\bar{B}^0)$. This shows that isospin symmetry needs to be broken for explaining the data. Otherwise, the puzzle would remain. In other words, the $B \rightarrow \pi K$ puzzle is solved by the broken isospin symmetry.

The isospin symmetry is broken by (i) the process-dependent factorization scale μ_i , and (ii) the process-dependent non-vanishing nonperturbative phases $\bar{\phi}_a, \bar{\phi}, \bar{\phi}_T$.

It is interesting to note that the mass differences $\Delta m_q = |m_d - m_u| \simeq 2.5$ MeV with $m_{u(d)}$ the up (down) quark's mass, $\Delta m_\pi = |m_{\pi^0} - m_{\pi^\pm}| \simeq 5$ MeV with $m_{\pi^0(\pi^\pm)}$ the pion's mass, $\Delta m_K = |m_{K^0} - m_{K^\pm}| \simeq 4$ MeV with $m_{K^0(K^\pm)}$ the kaon's mass, or $\Delta m_B = |m_{B^0} - m_{B^\pm}| \simeq 0.3$ MeV with $m_{B^0(B^\pm)}$ the $B^{0(\pm)}$ meson's mass can also break the isospin symmetry. The largest effect comes from the mass difference, $\Delta m_\pi \simeq 5$ MeV or $\Delta m_K \simeq 4$ MeV, which contribute about 5×10^{-5} of the ratio r .

To distinguish, we call the former as the “dynamic” and the latter as the “static” isospin symmetry breaking.

b. Nonperturbative Strong Phases The three nonperturbative strong phases $\bar{\phi}_a, \bar{\phi}, \bar{\phi}_T$ have a specific pattern in $B \rightarrow \pi K$ system as shown in Table II. The full strong phases, $\phi_a = \hat{\phi}_a + \bar{\phi}_a$, $\phi = \hat{\phi} + \bar{\phi}$, $\phi_T = \hat{\phi}_T + \bar{\phi}_T$, obey the pattern $|\phi_a| > |\phi| \simeq |\phi_T|$. A large negative ϕ_a is observed. Since these three phases are closely related to the weak angle γ , three phases could be redefined as $\Phi_a = \phi_a - \gamma$, $\Phi = \phi - \gamma$, $\Phi_T = \phi_T - \gamma$. From this respect, there exist three possibilities

1. The puzzle is solved by SM, if the phase factors ϕ_a, ϕ, ϕ_T are completely of strong interactions.
2. The puzzle is solved by NP, if the phase factors Φ_a, Φ, Φ_T completely come from NP effects.
3. Both of 1 and 2 are possible.

To clarify which scenario is correct relies on future studies.

VI. CONCLUSION

In this work, we have developed an effective method for analyzing the $B \rightarrow \pi K$ system by using the MQCDF model. The crucial roles are played by the phase factors $\bar{\phi}_a, \bar{\phi}, \bar{\phi}_T$. By the fitting strategy, we may determine their values definitely. It was found that their values depend on the decay modes. It is possible to extract a universal γ from the data, whose value is in good agreement with the world averaged value. The fit result was used to extract the weak angle β from the mixing induced CP asymmetry $S_{\pi^0 K_S^0}$. The extracted β is in a

good agreement with the world averaged value. From these evidences, our proposed model could completely solve the original puzzle defined in Sec.I.

The model could reconstruct the experimental data at the amplitude level as shown in Table VII. The isospin

symmetry of the $B \rightarrow \pi K$ system would be broken dynamically by strong interactions, such that the $B \rightarrow \pi K$ puzzle is solved. The application of our method to other decay processes is straightforward.

-
- [1] M. Battaglia, A. J. Buras, P. Gambino, A. Stocchi, D. Abbaneo, A. Ali, P. Amaral, V. Andreev, M. Artuso, E. Barberio, et al., ArXiv High Energy Physics - Phenomenology e-prints (2003), hep-ph/0304132.
 - [2] A. J. Buras, ArXiv High Energy Physics - Phenomenology e-prints (2005), hep-ph/0505175.
 - [3] A. J. Bevan, B. Golob, T. Mannel, S. Prell, B. D. Yabsley, H. Aihara, F. Anulli, N. Arnaud, T. Aushev, M. Beneke, et al., European Physical Journal C **74**, 3026 (2014), 1406.6311.
 - [4] C. Patrignani et al. (Particle Data Group), Chin. Phys. **C40**, 100001 (2016).
 - [5] M. Beneke, G. Buchalla, M. Neubert, and C. Sachrajda, Nuclear Physics B **606**, 245 (2001), ISSN 0550-3213.
 - [6] Y. Y. Keum, H.-N. Li, and A. I. Sanda, Phys. Rev. **D63**, 054008 (2001), hep-ph/0004173.
 - [7] H.-N. Li and S. Mishima, Phys. Rev. D **83**, 034023 (2011), 0901.1272.
 - [8] W. Bai, M. Liu, Y.-Y. Fan, W.-F. Wang, S. Cheng, and Z.-J. Xiao, Chinese Physics C **38**, 033101 (2014), 1305.6103.
 - [9] H.-n. Li, S. Mishima, and A. I. Sanda, Phys. Rev. **D72**, 114005 (2005), hep-ph/0508041.
 - [10] S. Khalil, A. Masiero, and H. Murayama, Phys. Lett. **B682**, 74 (2009), 0908.3216.
 - [11] A. J. Buras, R. Fleischer, S. Recksiegel, and F. Schwab, Phys. Rev. Lett. **92**, 101804 (2004), hep-ph/0312259.
 - [12] A. J. Buras, R. Fleischer, S. Recksiegel, and F. Schwab, Eur. Phys. J. **C32**, 45 (2003), hep-ph/0309012.
 - [13] A. J. Buras, R. Fleischer, S. Recksiegel, and F. Schwab, Nucl. Phys. **B697**, 133 (2004), hep-ph/0402112.
 - [14] M. Neubert, Journal of High Energy Physics **1999**, 014 (1999).
 - [15] C.-W. Chiang, M. Gronau, J. L. Rosner, and D. A. Suprun, Phys. Rev. **D70**, 034020 (2004), hep-ph/0404073.
 - [16] R. Fleischer, S. Jager, D. Pirjol, and J. Zupan, Phys. Rev. **D78**, 111501 (2008), 0806.2900.
 - [17] S. Baek and D. London, Phys. Lett. **B653**, 249 (2007), hep-ph/0701181.
 - [18] S. Baek, C.-W. Chiang, and D. London, Phys. Lett. **B675**, 59 (2009), 0903.3086.
 - [19] N. B. Beaudry, A. Datta, D. London, A. Rashed, and J.-S. Roux, Journal of High Energy Physics **2018**, 74 (2018), ISSN 1029-8479.
 - [20] M. Beneke, G. Buchalla, M. Neubert, and C. T. Sachrajda, Physical Review Letters **83**, 1914 (1999), hep-ph/9905312.
 - [21] M. Beneke and M. Neubert, Nuclear Physics B **675**, 333 (2003), hep-ph/0308039.
 - [22] G. Bell, Nuclear Physics B **822**, 172 (2009), 0902.1915.
 - [23] M. Beneke, T. Huber, and X.-Q. Li, Nuclear Physics B **832**, 109 (2010), 0911.3655.
 - [24] G. Bell, M. Beneke, T. Huber, and X.-Q. Li, Physics Letters B **750**, 348 (2015), 1507.03700.
 - [25] M. Neubert and B. D. Pecjak, Journal of High Energy Physics **2002**, 028 (2002).
 - [26] T.-W. Yeh, Chin. J. Phys. **46**, 535 (2008), 0802.1855.
 - [27] M. Imbeault, A. Datta, and D. London, International Journal of Modern Physics A **22**, 2057 (2007), hep-ph/0603214.
 - [28] A. J. Buras and L. Silvestrini, Nuclear Physics B **569**, 3 (2000), hep-ph/9812392.
 - [29] M. Gronau, D. Pirjol, and T.-M. Yan, Phys. Rev. **D60**, 034021 (1999), [Erratum: Phys. Rev.D69,119901(2004)], hep-ph/9810482.
 - [30] Y. Nir and H. R. Quinn, Phys. Rev. Lett. **67**, 541 (1991).
 - [31] M. Gronau, Phys. Lett. **B265**, 389 (1991).
 - [32] G. Buchalla, A. J. Buras, and M. E. Lautenbacher, Rev. Mod. Phys. **68**, 1125 (1996), hep-ph/9512380.
 - [33] A. J. Buras, in *Probing the standard model of particle interactions. Proceedings, Summer School in Theoretical Physics, NATO Advanced Study Institute, 68th session, Les Houches, France, July 28-September 5, 1997. Pt. 1*, 2 (1998), pp. 281–539, hep-ph/9806471.
 - [34] T.-W. Yeh, Chin. J. Phys. **46**, 649 (2008), 0712.2292.
 - [35] Y. Amhis, S. Banerjee, E. Ben-Haim, F. Bernlochner, A. Bozek, C. Bozzi, M. Chrzęszcz, J. Dingfelder, S. Duell, M. Gersabeck, et al., The European Physical Journal C **77**, 895 (2017), ISSN 1434-6052.
 - [36] William H. Press, Saul A. Teukolsky, William T. Vetterling, Brian P. Flannery, *Numerical Recipes (Third Edition)* (Cambridge University Press, 2010).
 - [37] D. W. Marquardt, Journal of the Society for Industrial and Applied Mathematics **11**, 431 (1963).
 - [38] M. Gronau, O. F. Hernández, D. London, and J. L. Rosner, Phys. Rev. D **52**, 6356 (1995), hep-ph/9504326.
 - [39] M. Gronau, O. F. Hernández, D. London, and J. L. Rosner, Phys. Rev. D **52**, 6374 (1995), hep-ph/9504327.
 - [40] D. Zeppenfeld, Z. Phys. **C8**, 77 (1981).
 - [41] A. J. Buras and R. Fleischer, Physics Letters B **341**, 379 (1995), hep-ph/9409244.
 - [42] A. J. Buras and R. Fleischer, Physics Letters B **360**, 138 (1995), hep-ph/9507460.
 - [43] R. Fleischer and T. Mannel, Phys. Rev. D **57**, 2752 (1998), hep-ph/9704423.
 - [44] M. Gronau and J. L. Rosner, Physics Letters B **572**, 43 (2003), hep-ph/0307095.
 - [45] H.-Y. Cheng, C.-K. Chua, and A. Soni, Phys. Rev. D **71**, 014030 (2005), hep-ph/0409317.

Figure 1. Three parton one loop diagrams for the vertex corrections of T^I are shown. The red gluon line means the gluonic parton g of the three parton $|q\bar{q}g\rangle$ state of the external M_2 meson state $|M_2\rangle$. The blue gluon line means the radiative loop gluons. The black box means the effective four quark operator. The other similar diagrams with the gluonic parton line connected to other external or internal parton lines to the vertex or penguin radiative loop corrections may also contribute. Similar three parton one loop diagrams for the T^{II} are not shown here. The figure refers to [34].

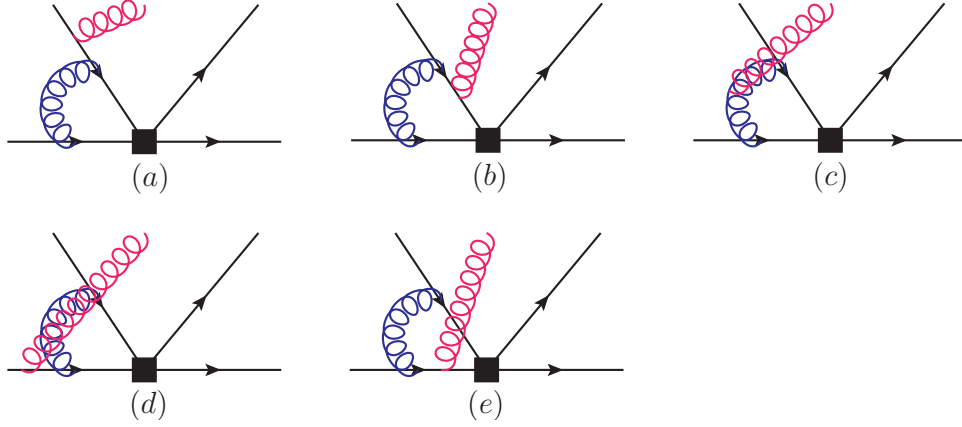


Table I. Input data [4] for numerical calculations. The errors are neglected. The reason refers to the text.

B meson parameters				
$\tau(B^0_d)(\text{ps})$	$\tau(B^-)(\text{ps})$	$m_{B^\pm}(\text{GeV})$	$m_{B^0}(\text{GeV})$	
1.52	1.64	5.28	5.28	
perturbative parameter				
$\Lambda_{\overline{MS}}^{(5)}(\text{GeV})$	$m_b(\text{GeV})$	$m_c(\text{GeV})$	$m_s(\text{GeV})$	
0.225	4.2	1.3	0.09	
decay constants and form factors				
$f_K(\text{GeV})$	$f_\pi(\text{GeV})$	$f_B(\text{GeV})$	$F_0^{B\pi}(0)$	$F_0^{BK}(0)$
0.16	0.13	0.2	0.28	0.34
CKM matrix elements				
$ V_{ub} $	$ V_{cb} $	$ V_{us} $	$ V_{cd} $	$ V_{cs} $
0.0037	0.042	0.23	0.22	0.97

Table II. Four factorization scales μ_i and the nonperturbative parts of the three strong phase parameters, $\bar{\phi}_a$, $\bar{\phi}$, and $\bar{\phi}_T$ are determined by a least squares fit method. The fitting strategy is described in the text. The upper and lower bounds of the parameters are determined by $\chi^2 \leq \sqrt{\nu}$ with ν the number of degrees of freedom. The fit determines the weak angle $\gamma = (72.1_{-5.8}^{+5.7})^\circ$.

decay modes	$\mu(\text{GeV})$	$\phi_a(\text{deg})$	$\phi(\text{deg})$	$\phi_T(\text{deg})$
$B^- \rightarrow \pi^- \bar{K}^0$	$4.55_{-0.25}^{+0.28}$	-50_{-56}^{+32}	NA	NA
$B^- \rightarrow \pi^0 K^-$	$5.25_{-0.37}^{+0.45}$	-50	$3.1_{-3.7}^{+3.6}$	NA
$\bar{B}^0 \rightarrow \pi^+ K^-$	$5.6_{-0.26}^{+0.28}$	-115.1	NA	16.3 ± 1.4
$\bar{B}^0 \rightarrow \pi^0 K^0$	$4.40_{-0.33}^{+0.35}$	-92	$23_{-40.6}^{+29.9}$	$23_{-40.6}^{+29.9}$

Table III. Hadronic parameters are calculated at $\mu_0 = 4.2_{-2.1}^{+4.2}$, $\mu_1 = (4.6 \pm 0.3)$, $\mu_2 = (5.3_{-0.4}^{+0.5})$, $\mu_3 = (5.6 \pm 0.3)$, $\mu_4 = (4.4_{-0.3}^{+0.4})$, $\mu_{av} = (5.0 \pm 1.4)$. The unit is in GeV. For simplicity, only central values are given for μ_i , $i = 1, \dots, 4$. The similar calculations up to twist-3 two parton NLO quoted from Ref.[5] are listed for comparisons. The \dagger term is calculated by using the values given in Ref.[5].

parameters	μ_0	Ref[5]	μ_1	μ_2	μ_3	μ_4	μ_{av}
$ P' (\text{eV})$	$51.4_{-10.3}^{+16.1}$	44.5^\dagger	50.0	47.7	46.7	50.6	$48.8_{-3.7}^{+6.0}$
$\epsilon_a(\%)$	1.9 ± 0.1	1.9 ± 0.1	1.9	1.9	1.9	1.9	1.9 ± 0.1
$\epsilon_{3/2}(\%)$	$22.7_{-6.4}^{+7.0}$	25.7 ± 4.8	23.5	24.9	25.6	23.2	$24.2_{-3.1}^{+2.5}$
$\epsilon_T(\%)$	$14.6_{-3.6}^{+4.0}$	22.0 ± 3.6	15.0	15.8	16.0	14.8	$15.4_{-1.8}^{+1.4}$
$q(\%)$	$60.1_{-4.4}^{+0.4}$	58.8 ± 6.7	60.2	60.4	60.4	60.2	$60.5_{-0.8}^{+0.2}$
$q_C(\%)$	$31.6_{-10.2}^{+3.2}$	8.3 ± 4.9	32.2	33.1	33.5	32.0	$33.0_{-3.0}^{+1.6}$
$\bar{\phi}_a(\text{deg})$	$21.5_{-2.5}^{+1.2}$	16.6 ± 5.2	21.3	20.8	20.6	21.4	$20.9_{-1.0}^{+1.1}$
$\bar{\phi}(\text{deg})$	$-10.2_{-1.7}^{+2.3}$	-10.2 ± 4.1	-10.4	-10.8	-11.0	-10.3	$-10.6_{-0.6}^{+0.9}$
$\bar{\phi}_T(\text{deg})$	$-6.8_{-2.6}^{+3.8}$	-6.2 ± 4.6	-7.2	-7.8	-8.0	-7.0	$-7.5_{-1.0}^{+1.5}$
$\omega(\text{deg})$	$0.4_{-0.7}^{+0.4}$	-2.5 ± 2.8	0.5	0.6	0.6	0.5	0.5 ± 0.2
$\omega_C(\text{deg})$	$-9.3_{-12.8}^{+4.4}$	-54.2 ± 44.2	-8.6	-7.5	-7.1	-8.0	$-7.9_{-3.2}^{+1.7}$

Table IV. Predictions and experimental data for branching ratios (10^{-6}) and direct CP asymmetries (10^{-2}).

Decay modes	Naive	Improved	S4[21]	pQCD[8]	Fit	PDG2016	HFAG2016
$Br(B^- \rightarrow \pi^- \bar{K}^0)$	$25.1_{-9.0}^{+18.2}$	$22.6_{-3.3}^{+5.9}$	20.3	$21.5_{-6.1}^{+8.0}$	$23.9_{-0.9-0.2}^{+0.8+0.0}$	23.7 ± 0.8	23.79 ± 0.75
$A_{CP}(B^- \rightarrow \pi^- \bar{K}_s^0)$	1.3 ± 0.1	1.3 ± 0.0	0.3	$0.38_{-0.140}^{+0.097}$	$-1.7_{-0.0-1.9}^{+0.0+1.7}$	-1.7 ± 1.6	-1.7 ± 1.6
$Br(B^- \rightarrow \pi^0 K^-)$	$14.7_{-4.7}^{+9.1}$	$13.5_{-5.1}^{+3.0}$	11.7	$12.5_{-3.4}^{+4.5}$	$13.1_{-0.6-0.1}^{+0.5+0.0}$	12.9 ± 0.5	$12.94_{-0.51}^{+0.52}$
$A_{CP}(B^- \rightarrow \pi^0 K^-)$	$7.8_{-2.6}^{+2.9}$	$8.4_{-1.3}^{+1.0}$	-3.6	2.2 ± 2.1	$3.6_{-0.2-2.5}^{+0.3+2.5}$	3.7 ± 2.1	4.0 ± 2.1
$Br(\bar{B}^0 \rightarrow \pi^+ K^-)$	$23.6_{-8.1}^{+15.9}$	$21.4_{-3.0}^{+5.2}$	18.4	$17.7_{-4.9}^{+6.4}$	$19.9_{-0.6-0.0}^{+0.5+0.0}$	19.6 ± 0.5	$19.57_{-0.52}^{+0.53}$
$A_{CP}(\bar{B}^0 \rightarrow \pi^+ K^-)$	$4.4_{-2.0}^{+2.3}$	$4.9_{-1.1}^{+0.8}$	-4.1	-6.5 ± 3.1	$-8.2_{-0.0-0.7}^{+0.0+0.7}$	-8.2 ± 0.6	-8.2 ± 0.6
$Br(\bar{B}^0 \rightarrow \pi^0 K^0)$	$10.2_{-3.8}^{+7.9}$	$9.2_{-1.4}^{+2.5}$	8.0	$7.4_{-2.1}^{+2.7}$	$10.0_{-0.5-0.0}^{+0.5+0.4}$	9.9 ± 0.5	9.93 ± 0.49
$A_{CP}(\bar{B}^0 \rightarrow \pi^0 K^0)$	$-3.4_{-1.8}^{+1.4}$	$-3.7_{-0.7}^{+0.8}$	0.8	$-7.9_{-1.1}^{+0.9}$	$-1.0_{-0.1-12.3}^{+0.1+8.3}$	-1 ± 10	-1 ± 10

Table V. The different terms of the direct CP asymmetries. The index i denotes the decay mode: $i = 1$ for $B^- \rightarrow \pi^- K^0$, $i = 2$, for $B^- \rightarrow \pi^0 K^-$, $i = 3$ for $\bar{B} \rightarrow \pi^- K^+$, and $i = 4$ for $\bar{B}^0 \rightarrow \pi^0 K^0$. The other columns refer to the text.

i	N_i	1st term (10^{-3})	2nd term (10^{-3})	3rd term (10^{-3})	4th term (10^{-3})	$A_{CP}(10^{-3})$
1	1.98	-8.7	0	0	0	-17.2
2	1.65	-8.8	31.9	-1.0	0.4	36.9
3	1.94	-18.0	-21.9	-1.0	-1.0	-81.3
4	2.25	-8.3	-0.8	1.6	2.0	-12.3

Table VI. Experimental data and the QCDF predictions for ratios R , R_c , R_n .

Observable	2007[17]	2016[4]	Fit	S4	Naive	Improved
R	0.89 ± 0.04	0.89 ± 0.05	0.87 ± 0.04	0.89	0.92 ± 0.67	0.91 ± 0.26
R_c	1.10 ± 0.07	1.09 ± 0.06	1.10 ± 0.07	1.15	1.17 ± 1.12	1.19 ± 0.55
R_n	1.00 ± 0.07	0.99 ± 0.06	1.00 ± 0.06	1.15	1.16 ± 1.19	1.16 ± 0.42

Table VII. Amplitudes calculated according to the Improved and Fit data. Only uncertainties from the scale variables μ_{av} and μ_i , $i = 1, \dots, 4$, are included.

decay modes	Improved	Fit
$A(B^- \rightarrow \pi^- K^0)(\text{eV})$	$(49.4 \pm 6.0)e^{-i173^\circ}$	$(50.0 \pm 1.1)e^{-i173^\circ}$
$A(B^- \rightarrow \pi^0 K^-)(\text{eV})$	$(39.5 \pm 3.8)e^{i18^\circ}$	$(38.0 \pm 0.9)e^{i19^\circ}$
$A(\bar{B}^0 \rightarrow \pi^- K^+)(\text{eV})$	$(50.8 \pm 5.5)e^{i15^\circ}$	$(45.8 \pm 0.7)e^{i17^\circ}$
$A(\bar{B}^0 \rightarrow \pi^0 K^0)(\text{eV})$	$(31.9 \pm 4.2)e^{-i177^\circ}$	$(33.7 \pm 1.0)e^{-i179^\circ}$
$A(B^- \rightarrow \pi^- K^0) + \sqrt{2}A(B^- \rightarrow \pi^0 K^-)$	$(12.0 \pm 8.0)e^{i70^\circ}$	$(11.5 \pm 1.7)e^{i84^\circ}$
$A(\bar{B}^0 \rightarrow \pi^- K^+) + \sqrt{2}A(\bar{B}^0 \rightarrow \pi^0 K^0)$	$(11.5 \pm 8.0)e^{i70^\circ}$	$(13.1 \pm 1.6)e^{i107^\circ}$
r	$(1.04 \pm 1.0)e^{i0.4^\circ}$	$(0.87 \pm 0.15)e^{-i23^\circ}$